STUDIA UNIVERSITATIS BABEŞ-BOLYAI BIOLOGIA, 71, 1, 2026 (p. 71-100)
doi:10.24193/subbbiol.2026.1.05

Leveraging the power of computational immunology to develop a novel couplet mRNA vaccine concatenating conserved epitopes of monkeypox virus antigens

Leana Rich Herrera-Ong

Department of Biochemistry and Molecular Biology, College of Medicine, University of the Philippines Manila, Manila City, Philippines
E-mail: lmherrera2@up.edu.ph

Article history: Received 9 August 2025; Revised 2 December 2025; Accepted 16 March 2026; Available online 25 June 2026

Abstract. The monkeypox (Mpox) disease was declared as a Public Health Emergency of International Concern (PHEIC) in 2022 and in 2024. Currently, there are no Mpox-specific vaccines and antiviral drugs for the treatment of Mpox. This study developed a novel couplet mRNA vaccine through immunoinformatics tools and databases. Highly conserved sequences of nine Mpox antigens were identified and utilized for T-cell and B-cell epitope mapping. Using data obtained from experimentally validated epitopes, the potential immunogenicity of predicted T-cell epitopes was evaluated. Peptides that may cause cross-reactivity, toxicity, and allergic reactions were excluded. The population coverage of candidate epitopes was also estimated. Epitopes were arranged and adjoined to form the mRNA constructs, aiming to direct its processing either to exogenous or endogenous pathways, while maximizing cleavage scores to produce the desired peptides. Conservancy analysis revealed that the nine Mpox target antigens A29L, A35R, A42R, B6R, E8L, F13L, H3L, L1R, and M1R are highly conserved. After the exclusion of potentially harmful and non-immunogenic peptides, 559 CD4+ and 104 CD8+ T-cell epitopes remained. The couplet mRNA constructs encode potentially immunogenic T-cell epitopes and accessible B-cell epitopes of multiple Mpox antigens that can be expressed and processed to generate the desired peptide sequences in humans. Estimated population coverage for mTcPox and mBThPox

constructs are 77.67% and 81.81%, respectively. This study developed a novel couplet mRNA Mpox vaccine design containing highly conserved, immunogenic epitopes, with acceptable safety profile. Further *in vitro*, animal, and clinical studies are anticipated for human applications.

Keywords: epitope; immunoinformatics; monkeypox; Mpox; mRNA vaccines

Introduction

The World Health Organization (WHO) declared the monkeypox (Mpox) virus outbreak—a zoonotic disease—as a Public Health Emergency of International Concern (PHEIC) twice: first in 2022 and again in 2024 (Sagdat *et al*., 2024). As of 2025, the global prevalence of Mpox continues to rise, particularly in African countries, with imported cases increasingly reported in other regions. Individuals with compromised immune systems and those with multiple sexual partners face a heightened risk of infection. Between January 2022 and March 2025, a total of 137,892 confirmed cases and 317 deaths were reported across 132 countries, with the majority of fatalities occurring in African nations (Yadav *et al*., 2025).

Two major clades of the Mpox virus—Clade I and Clade II—are currently circulating worldwide. Clade II has been primarily responsible for the widespread outbreak from 2022 to 2025. More recently, the emergence of Mpox Clade Ib in Southeast Asia (SEA) has raised concerns, especially for countries already grappling with Clade IIb since 2022 (A *et al*., 2025). The mortality rate of Mpox varies depending on the viral strain, ranging from 10% to 15% (Bogacka *et al*., 2025).

The natural reservoirs of the Mpox virus are believed to be primates and certain rodent species native to Africa. Human-to-human transmission occurs through direct contact with mucous membranes, body fluids, tissues, or respiratory droplets from infected individuals (Beeson *et al*., 2023). The severity of Mpox infection is influenced by the patient's immune status, the specific viral strain involved, and the presence of complications. The virus typically enters the body through skin lesions or mucous membranes and then disseminates systemically. The latent period lasts up to two weeks, during which infected individuals remain asymptomatic and show no visible lesions. Following this phase, symptoms such as fever, muscle pain, headache, and lymphadenopathy emerge and persist for approximately three days. Subsequently, a rash develops over a span of two to four weeks, progressing from papules to pustules and vesicles. These lesions eventually crust over and heal, often leaving scars (Zahmatyar *et al*., 2023).

Mpox virus belongs to the family Poxviridae and the genus *Orthopoxvirus*. It is characterized by its oval morphology and a dumbbell-shaped nucleocapsid encased in lipid-containing particles. The viral genome is approximately 197 kb in size and encodes around 190 proteins. The virus exists in two distinct forms: extracellular enveloped virions (EEV) and intracellular mature virions (IMV). IMVs have a single membrane and enter host cells via fusion and endocytosis, being released upon cell lysis. EEVs, which possess a double membrane, attach to host mucous membranes through glycosaminoglycans (GAGs) and enter via membrane fusion (Lu *et al*., 2023).

Targeting EEV surface proteins such as B6R and A35R may help reduce viral transmission. F13L, another EEV protein, is embedded within the viral envelope and is essential for the formation of extracellular viral particles (Callaby *et al*., 2025). IMV-associated antigens include A29R, H3L, E8L, L1R, and M1R. A29R facilitates viral fusion, replication, and egress. H3L enhances viral binding to host cells, increasing infectivity. E8L promotes surface attachment and entry, while L1R and M1R contribute to viral entry, assembly, and neutralization. A42R, a profilin-like protein, interacts with actin filaments, but its role in Mpox pathogenesis remains unclear (Sagdat *et al*., 2024). Taken together, these antigens play critical roles in Mpox virulence and represent promising targets for antiviral drug and vaccine development.

Smallpox vaccines approved for Mpox offer only partial efficacy, and viral transmission continues due to the lack of Mpox-specific vaccines or drugs. Current antivirals—tecovirimat, brincidofovir, and cidofovir—were originally developed for smallpox (Bogacka *et al*., 2025). Advancing the development of Mpox-targeted therapeutic agents is therefore essential. Immunoinformatics provides powerful tools for identifying and designing vaccine components (Rawat *et al*., 2023). This study aims to develop a novel couplet Mpox mRNA vaccine using advanced immunoinformatic techniques. The vaccine includes specific, conserved, and immunogenic B-cell and T-cell epitopes targeting multiple Mpox antigens. Each epitope is directed to either endogenous or exogenous pathways to optimize immune processing. The couplet mRNA sequences are designed for enhanced expression in human cells and improved molecular stability, making them suitable for future immunotherapeutic applications.

Materials and methods

Identification of conserved sequences in Mpox antigens

The protein sequences of Mpox antigens were obtained from the National Center for Biotechnology Information (NCBI) on June 5, 2025. The full lengths of A29L, A35R, A42R, B6R, E8L, F13L, H3L, L1R, and M1R are 110, 181, 133, 317, 304,

372, 324, 152 and 250 amino acid residues, respectively. Redundant sequences were removed in the Galaxy CD-HIT server (https://usegalaxy.eu/?tool_id=cd_hit). Variable positions were identified and masked in Protein Variability Server (http://imed.med.ucm.es/PVS/) using the Shannon variability threshold ≤ 0.1 and fragments with at least 6 residues.

Mapping of CD8+ and CD4+ epitopes

Cytotoxic T-cell epitopes were identified using the recommended algorithm in IEDB–NetMHCIPan 4.1 BA (https://nextgen-tools.iedb.org/pipeline?tool=tc1). The IC_{50} threshold used to classify good binders is < 500 nM (Reardon *et al*., 2021). To increase prediction accuracy, the thresholds for proteasome and TAP scores were set to > 1.0 (Olotu *et al*., 2021). Helper T-cell epitopes were mapped using IEDB NetMHCIIPan 4.1 BA, with IC_{50} < 500 nM to identify good binders. The Uniprot database (https://www.uniprot.org/) was consulted to determine known residues in the target antigens with post-translational modifications (PTM). Epitopes with PTM residues were excluded from the set of T-cell epitopes to be assessed in subsequent steps.

Assessment of potentially immunogenic helper and cytotoxic T-cell epitopes

The set of mapped cytotoxic T-cell epitopes were further filtered using three different state-of-the-art immunogenicity tools. DeepImmuno (DIm) uses a convolutional neural network (CNN) algorithm to predict the immunogenicity of MHC–peptide pairs (https://deepimmuno.research.cchmc.org/). DIm was found to have high average auROC (0.85) and auPR (0.81) (Li *et al*., 2021). The T cell class I p-MHC immunogenicity predictor (CIImm) in IEDB (http://tools.iedb.org/immunogenicity/) assesses immunogenicity by providing an immunogenicity score calculated as a position-dependent weighted sum of the non-anchor amino acids of the neoantigen amino acid sequence (Nibeyro *et al*., 2023). PRIME 2.0 is another state-of-the-art immunogenicity tool that combines affinity predictions with TCR-recognition propensity (http://prime.gfellerlab.org). Rank is provided and a non-immunogenic peptide receives a score of zero (Gfeller *et al*., 2023). Currently, there is no consensus threshold value to identify immunogenic epitopes. In general, the higher the immunogenicity score, the higher the probability of an epitope being immunogenic (Nibeyro *et al*., 2023). To create a more stringent standard in this study, the structures of five experimentally validated cytotoxic T-cell epitopes with their MHC I binders, were obtained and utilized as positive references for the immunogenicity analysis of predicted cytotoxic T-cell epitopes. These five experimentally validated CD8+ T-cell epitopes are:

HPV.16 E7 peptide LLMGTLGIV (6APN), HIV epitope SLYNTVATL (5NMD), SARS-CoV-2 spike-derived peptide YLQPRTFLL (7RTD), SARS-CoV-2 spike-derived peptide K417T mutant TIADYNYKL (7UM2), and SARS-CoV-2 spike-derived peptide YIWLGFIAGL (7UR1). The immunogenicity scores of experimentally validated CD8+ T-cell epitopes were determined in DIm, CIIm and PRIME 2.0. This study excluded all predicted cytotoxic T-cell epitopes with immunogenicity scores lower than any of the lowest immunogenicity scores of the 5 positive references.

The release of interferon-gamma (IFN-gamma) is a hallmark of Th1 response that is critical to mitigate intracellular pathogens, such as Mpox viruses. IFN-epitope server (http://crdd.osdd.net/raghava/ifnepitope/) was utilized to identify which among the predicted CD4+ T-cell epitopes can potentially induce IFN-γ. The study selected the hybrid algorithm which combines the advantages of SVM-based and motif-based techniques (Dhanda *et al.,* 2013). IL4pred server (https://webs.iiitd.edu.in/raghava/il4pred/predict.php) was utilized to identify helper T-cell epitopes that can potentially induce IL4. Using motif information and amino acid pairs, the accuracy of this method is found to be 75.76% (Nebangwa *et al.,* 2024). With an SVM threshold of 2.0, the hybrid SVM-based and motif-based technique was employed to identify IL4-inducing CD4+ epitopes. The remaining epitopes were further analyzed for potential cross-reactivity, toxicity, and allergenicity.

Mapping of B-cell epitopes in the extracellular enveloped virus proteins of Mpox

Mpox B6R and A35R are two most accessible extracellular enveloped virus (EEV) proteins that play pivotal roles in cell attachment and effective spreading. EEV is an enveloped form of virus released from the cell that is capable of infecting other cells. Thus, peptide sequences of B6R and A35R were retrieved to identify potential B-cell epitopes. ABCpred (https://webs.iiitd.edu.in/raghava/abcpred/index.html) tool, together with six other well-established linear B-cell epitope prediction tools (Bepipred Linear Epitope Prediction 2.0, Chou & Fasman Beta-Turn Prediction, Emini Surface Accessibility Prediction, Karplus & Schulz Flexibility Prediction, Kolaskar & Tongaonkar Antigenicity, and Parker Hydrophilicity Prediction) in IEDB (http://tools.iedb.org/bcell/) were applied to map B-cell epitopes using default thresholds. Using 6-kmer consensus sequences, peptide sequences that overlap in at least 5 different tools were included. Resulting epitopes that are located in the transmembrane and internal regions were removed. The transmembrane, internal and external domains of each sequence were identified using the Interproscan tool (https://www.ebi.ac.uk/interpro/search/sequence/). B-cell epitopes with variable residues and PTMs were also excluded. The remaining

B-cell epitopes were further evaluated for potentially cross-reactive, allergenic, and toxic peptides. Lastly, overlapping B-cell epitopes per antigen were integrated into a single peptide sequence.

Exclusion of potentially cross-reactive, toxic and allergenic T-cell and B-cell epitopes

All the epitopes were thoroughly inspected using the BLASTP tool (https://blast.ncbi.nlm.nih.gov/Blast.cgi?PAGE=Proteins), to exclude peptides having 100% coverage and 100% identity with at least 7 adjacent residues in any human protein sequence from the Reference Protein database (refseq) in NCBI. Models, non-redundant RefSeq proteins, and uncultured/environmental sample sequences were excluded in the search to avoid unrelated sequences. The ToxinPred3.0 server (https://webs.iiitd.edu.in/raghava/toxinpred3/) was used to assess potentially toxic peptides. Default threshold score 0.38 was applied in the Hybrid (ET+MERCI) method. This technique demonstrated superiority, achieving 0.98 area under the ROC curve (AUROC) and Matthews correlation coefficient (MCC) 0.81 (Rathore *et al*., 2024). Potential allergens were also identified and excluded using two highly accurate methods: AllerCatPro 2.0 (https://allercatpro.bii.a-star.edu.sg/) and pLM4Alg (https://f6wxpfd3sh.us-east-1.awsapprunner.com). On validation dataset, AllerCatPro2.0 outperformed other benchmark methods for predicting allergenic proteins with maximum performance of area under the curve (AUC) 0.98 with MCC 0.85 on the validation dataset (Sharma *et al.,* 2021). The pLM4Alg tool, another state-of-the-art model, achieved accuracy of 93.4 to 95.1%, MCC 0.869 to 0.902, and AUC scoring of 0.981 to 0.990 (Du *et al.,* 2024). Epitopes identified as non-allergens in both tools were included in the list of candidate epitopes.

Estimation of the population coverage of candidate T-cell epitopes

The cumulative and the individual coverages of candidate CD4+ and CD8+ T-cell epitopes were estimated in world and in regions highly burdened by Mpox, including: North, West, East, South, and Central Africa. The population coverage was also determined for the Southeast Asian (SEA) region. Cumulative population coverage of selected and adjoined CD4+ and CD8+ T-cell epitopes encoded in the mRNA constructs were also calculated to estimate the percentage that can be covered by each mRNA vaccine construct.

Molecular docking of the selected candidate T-cell epitopes

For each Mpox antigen, the epitope with the highest population coverage was selected to be encoded in the mRNA constructs. Using IC_{50} as a metric of binding affinity, the weakest HLA binder was chosen for molecular docking with its respective epitope. The PDB structures of the following HLA molecules were obtained from the RCSB Protein Data Bank (https://www.rcsb.org/). These include: HLA-DRB11501, HLA-DRB10401, HLA-B3501, HLA-B5801, HLA-B5701, HLA-B4001, HLA-A2402, HLA-A0301, HLA-A1101, HLA-B5301, and HLA-B1501, with PDB ID 1bx2, 5ni9, 4lnr, 5vwh, 6bxq, 6iex, 6xqa, 7l1b, 7m8t, 7r7v, and 8elh, respectively. Unrelated hetero atoms were removed from the PDB structures of the HLAs. The selected candidate CD4+ and CD8+ T-cell epitopes were docked with the predicted HLA binders using the GalaxyPepDock server (https://galaxy.seoklab.org/cgi-bin/submit.cgi?type=PEPDOCK). Resulting PDB structures of complex with estimated accuracy below 1.0 were further refined in the GalaxyRefineComplex tool (https://galaxy.seoklab.org/cgi-bin/submit.cgi?type=COMPLEX). The dissociation constant (K_D) and the Gibbs free energy change (ΔG_{bind}) of complex formation at 37^0C were also calculated in the Prodigy webserver (https://rascar.science.uu.nl/prodigy/).

Design and evaluation of the mTcPox RNA sequence

The selected candidate CD8+ epitopes were adjoined to form the mTcPox construct wherein the first residue in the first epitope of the construct begins with methionine. Subsequent epitopes were arranged and adjoined in order to maximize the immunoproteosome cleavage scores; thereby, increasing the chance for the desired CD8+ epitope sequences to be produced upon intracellular immunoproteosome cleavage. The Proteasome Cleavage Prediction Server (iPCPS) with a threshold score of 0.5 was used for this purpose (http://imed.med.ucm.es/Tools/pcps/index.html). The relevant physicochemical properties of the product of mTcPox open reading frame (ORF) were determined using the Protparam webserver (https://web.expasy.org/protparam/). The ORF sequence of mTcPox was reverse translated to RNA sequence in the EMBOSS Backtranseq tool and optimized for translation in *Homo sapiens* (https://www.ebi.ac.uk/jdispatcher/st/emboss_backtranseq). Essential sequences were added to finally form the RNA sequence of mTcPox construct. This study suggests the use of the conventional 5' cap 1 (m7GpppN1m) in the 5' end of the 5' untranslated region (5' UTR). The leader sequence (GAAAAAAAAAAAAGGC) of the 5' UTR is consist of poly A (12 nt), Kozak consensus sequence and the human beta globin sequence (ACATTTGCTTCTGACACAACTGTGTTCACTAGCAACCTCAAACAGACACC), in order to

increase translation efficiency and prevent secondary structure formation at the 5' end (Dhungel *et al,* 2017). Sequence of 5' UTR human beta-globin (1-53) was retrieved from NCBI (NM_000518.5). The reverse translated ORF sequence of mTcPox was added after the 5' UTR region. The ORF sequence is followed by a 3' UTR sequence, which is consist of a stop codon (TAA) and the *Homo sapiens* beta-globin 3' UTR sequence (GCTCGCTTTCTTGCTGTCCAATTTCTATTAAAGGTTCCTTTGTTCCCTAAGTCCA ACTACTAAACTGGGGGATATTATGAAGGGCCTTGAGCATCTGGATTCTGCCTAAT AAAAAACATTTATTTTCATTGCAA). The beta-globin sequence (492 to 628) of the 3' UTR was also obtained from NCBI (NM_000518.5). Lastly, an ideal length (100 nt) of poly (A) tail was added for synthesizing therapeutic mRNA. This study also suggests the replacement of uridine by pseudouridine (N1-methylpseudouridine) to reduce immune reaction toward mRNA (Ho *et al*., 2024). It is also essential to increase the GC content of the mRNA construct for greater stability and better protein translation efficiency. The translation efficiency of ORF sequence can be estimated using Codon Adaptation Index (CAI). The CAI and the GC content of the optimized ORF were calculated using the VectorBuilder Codon Optimization tool for expression in humans (https://en.vectorbuilder.com/tool/codon-optimization.html). RNA Folding Form v2.3 (https://www.unafold.org/mfold/applications/rna-folding-form-v2.php) was used to calculate and predict the minimum free energy for the optimal secondary structure of mTcPox RNA sequence at 37 degrees Celsius. The GU pairs and isolated bases were avoided at the end of the helices.

Design and evaluation of the mBThPox RNA sequence

The mRNA construct of MBThPox, containing the adjoined B-cell and helper T-cell epitopes, was designed to be translated and secreted for the binding of B-cell epitopes to B-cell receptors (BCRs) and the processing of CD4+ epitopes through the exogenous pathway. The *Homo sapiens* renin signal sequence (MDGWRRMPRWGLLLLLWGSCTFG) was used as the first stretch of amino acid sequence in the ORF of the construct. Selected candidate CD4+ epitopes were added next to the renin signal sequence. The helper T-cell epitopes were arranged in order to maximize the probability of cleavage by proteases known to generate and process CD4+ epitopes (cathepsins D, L, and G). The cleavage score of C-terminus residue of each epitope was determined using the ProsperousPlus tool (http://prosperousplus.unimelb-biotools.cloud.edu.au/index.php/prediction). B-cell peptides were added in the last part of the construct. These peptides cover the overlapping candidate linear B-cell epitopes mapped in this study. The peptides were linked using KK and AAY

linkers to enhance the likelihood of recognition of the candidate B-cell epitopes within the model protein structure of the construct. The signal cleavage site of mBThPox ORF sequence was further assessed through the SignalIP 6.0 server (https://services.healthtech.dtu.dk/services/SignalP-6.0/), to ensure that the renin signal sequence in the construct is recognized and cleaved between positions 23 and 24 by signal peptidase I. The probability that the antigen protein will not be GPI-anchored was also predicted in the NetGPI 1.1 webserver (https://services.healthtech.dtu.dk/services/NetGPI-1.1/). These steps are crucial for the translated product of the mBThPox vaccine to be secreted and not to be anchored within the cell membrane.

The adjoined linear B-cell epitopes in the translated protein structure of mBThPox must be located in disordered and paratope-accessible regions for effective BCR binding and recognition. This study determined the secondary structure composition of the vaccine in order to identify the positions of random coil regions using the GOR4 webserver tool (https://npsa-prabi.ibcp.fr/cgi-bin/npsa_automat.pl?page=npsa_gor4.html). The protein structure model of mBThPox was generated using the GalaxyTBM tool (https://galaxy.seoklab.org/cgi-bin/submit.cgi?type=TBM) in order to assess the accessibility of adjoined linear B-cell epitope. The model structure was further refined in the GalaxyRefine2 webserver (https://galaxy.seoklab.org/cgi-bin/submit.cgi?type=REFINE2), and the generated structure model was inspected through iCn3D tool (https://www.ncbi.nlm.nih.gov/Structure/icn3d/). To validate its quality, the percentage of residues lying within the favored and the disallowed regions were calculated using the Wenglab Ramachandran Plot sever (https://bu.wenglab.org/rama/). The quality factor for non-bonded atomic interactions (ERRAT score) was determined in the UCLA SAVESv.6.0 server (https://saves.mbi.ucla.edu/). The accessibility of adjoined B-cell epitopes in the structure of the translated product of mBThPox was investigated in Ellipro (http://tools.iedb.org/ellipro/). The physicochemical properties of the translated product were also determined using the Protparam tool (https://web.expasy.org/protparam/).

The ORF sequence of mBThPox was reverse translated and optimized in the EMBOSS Backtranseq tool. Similar to the steps conducted to generate the final mRNA sequence of mTcPox, essential elements for mRNA translation were also added to the reverse-translated ORF sequence of mBThPox. The percentage GC content and translation efficiency of its ORF sequence was determined, and the minimum free energy of the optimal secondary structure of mBThPox nucleotide sequence was also calculated.

Results

The highly conserved antigens of Mpox virus

The validity for the use of Shannon variability index requires at least 100 protein sequences per antigen. The number of sequences retrieved from NCBI for A29L, A35R, A42R, B6R, E8L, F13L, H3L, L1R, and M1R are 564, 558, 564, 562, 568, 567, 571, 562 and 562, respectively. The positions of variable residues in Mpox antigens are listed in Supplementary File 1.

The candidate CD8+ and CD4+ T-cell epitopes of Mpox antigens

This study predicted and filtered CD8+ and CD4+ T-cell epitopes according to the set of criteria described in the methodology. Processing with MHC I-IEDB Recommend NetMHCIPan and MHC II-IEDB Recommend NetMHCIIPan 4.1 BA resulted in T-cell epitopes with IC_{50} values ranging from 4.6 to 499.99 and 2.9 to 499.1 nM, for CD4+ and CD8+ epitopes, respectively. Five experimentally validated CD8+ T-cell epitopes were obtained and utilized to provide threshold scores with the aid of three state-of-the-art immunogenicity tools. Table 1 indicates the threshold scores employed in filtering CD8+ T-cell epitopes which are 0.566, -0.104, and 0.043, using DIm, CIIm, and PRIME, respectively. Predicted cytotoxic T-cell epitopes with scores less than any of the 3 thresholds were excluded. Mapped CD4+ T-cell epitopes classified as non-IL4 and/or non-IFN-gamma inducers were also excluded in this study.

Table 1. Immunogenicity scores of experimentally validated cytotoxic T-cell epitopes

CD8+ T-cell epitope	HLA I allele	DIm score	CIIm score	PRIME score
LLMGTLGIV	A*0201	0.820	0.386	0.043
SLYNTVATL	A*0201	0.925	0.131	0.267
YLQPRTFLL	A*0201	0.811	0.125	0.187
TIADYNYKL	A*0201	0.566	0.111	0.212
YIWLGFIAGL	A*0201	0.759	-0.104	0.612
Immunogenicity thresholds		*0.566*	*-0.104*	*0.043*

Upon manual and thorough inspection, some of the predicted epitopes showed significant hits with particular human proteome sequences. These include: spermatogenesis-associated protein 32 (A29L); inaD-like protein isoform 2 (A35R); breast cancer type 2 susceptibility protein isoform 1, and sister chromatid cohesion protein PDS5 homolog A isoform 1 (B6R); cilia- and flagella-associated protein 43, and von Willebrand factor D and EGF domain-containing protein isoform 1 precursor (E8L); E3 SUMO-protein ligase EGR2 isoform a, early growth response protein 3 isoform 1, neuron navigator 3 (F13L); S phase cyclin A-associated protein in the endoplasmic reticulum isoform a, dimethyladenosine transferase isoform 1, and rho guanine nucleotide exchange factor 26 isoform 1 (H3L); and apoptosis-inducing factor short isoform 3, mucin-5B precursor, and E3 ubiquitin-protein ligase (M1R) with the predicted CD4+ T-cell epitopes. One CD8+ B6R epitope was found to have a significant hit with human GPI mannosyltransferase 4. After the exclusion of potentially cross-reactive, allergenic and toxic peptides, a total of 559 CD4+ and 104 CD8+ epitopes remained; and hereby, classified as candidate T-cell epitopes. The IC_{50} value range for the set of candidate CD4+ and CD8+ T-cell epitopes, and the number of candidate epitopes for each Mpox antigen, are also found in Supplementary File 2.

The candidate B-cell epitopes of Mpox EEV proteins

The predicted external regions of Mpox EEV proteins A35R and B6R are positions 58 to 181, and 20 to 227, respectively. Using only the external sequences, consensus B-cell epitopes were determined by utilizing 7 different B-cell epitope mapping tools. Epitopes containing variable and PTM residues were excluded. After filtering out potentially cross-reactive, allergenic, and toxic epitopes, a total 18 (12 for A35R and 6 for B6R) epitopes remained in the list of candidate Mpox B-cell epitopes. Table 2 shows three peptide sequences (P1 to P3) spanning the 18 candidate B-cell epitopes. These three peptides were included in the mRNA vaccine construct proposed by the study. P1 and P2 are found in positions 146-178 and 115-143 of Mpox A35R, respectively. P3 is in position 23-45 of Mpox B6R.

Table 2. The peptide sequences of P1, P2, and P3 with the candidate B-cell epitopes

Antigen	Peptide	Code	Position	Residues	B-cell epitopes overlap
A35R	DYVEDTWGS DGNPITKTTS DYQDSDVSQE VRKY	P1	146-178	33	TKTTSDYQDSDVSQEV DTWGSDGNPITKTTSDYQDSDVSQE VRKYFC TWGSDGNPITKTTSDYQDSDVSQEV ITKTTSDYQDSDV EDTWGSDGNPITKTTSDYQDSDVS DYVEDTWGSDGNPITKTTSDYQDS DVSQEVRKY EDTWGSDGNPITKTTS
	DYKSFEDAKA NCAAESSTLP NKSDVLTTW	P2	115-143	29	STLPNKSDVLTT AESSTLPNKSDVLTTW STLPNKSD ESSTLPNKSDVL DYKSFEDAKANCAAESSTLPNKSDV
B6R	VPTMNNAKLT STETSFNDKQ KVT	P3	23-45	23	PTMNNAKLTSTETSFN VPTMNNAKLTSTETSFNDKQKV PTMNNAKLTSTETSFNDKQKV AKLTSTETSFNDKQKV KLTSTETSFNDKQKVT LTSTETSFNDK

Candidate cytotoxic and helper T-cell epitopes cover significant percentage of populations

The candidate epitopes encoded by the couplet mRNA constructs were selected according to the highest percentage of population it can cover. Table 3 presents the selected candidate CD4+ and CD8+ T-cell epitopes, with the IC_{50} range values for their HLA binders. The estimated world population coverage of the set of candidate CD8+ and CD4+ epitopes are 77.67% and 81.81%, respectively. Consequently, the cumulative population coverage of epitopes in the mTcPox construct is 77.67% and 81.81% for the mBThPox mRNA construct (Table 4), as epitopes with the highest population coverage per antigen were selected for inclusion. The individual population coverage of each T-cell epitope in selected regions, where Mpox is currently prevalent, are also indicated in Table 4. The data for some HLA II alleles were not available and therefore not included in the calculation. These alleles include:

HLA-DPA1*03:01/DPB1*04:02, HLA-DPA1*02:01/DPB1*05:01, HLA-DQA1*04:01/DQB1*04:02, HLA-DQA1*05:01/DQB1*02:01, HLA-DRB4*01:01, HLA-DPA1*02:01/DPB1*01:01, HLA-DQA1*01:02/DQB1*06:02, HLA-DRB3*02:02, HLA-DPA1*01:03/DPB1*04:01, HLA-DPA1*02:01/DPB1*14:01, HLA-DPA1*01:03/DPB1*02:01, HLA-DQA1*05:01/DQB1*03:01, and HLA-DRB5*01:01.

The set of CD8+ epitopes can cover as high as 92.77% of the population in West Africa, while the set of CD4+ epitopes can cover as high as 81.81% of the world population. The lowest percentage of populations covered by CD8+ and CD4+ epitope sets are 77.67% and 32.1%, in the world and in South Africa, respectively.

Table 3. The peptide sequence and the IC_{50} range values of selected T-cell epitopes

Antigen	T-cell	Epitope	IC_{50} range (nM)
A29L		LAIPATEFF	14.5—139.6
A35R		TSVFSATVY	136.1—155.6
A42R		IARTHTALIF	78.3—175.1
B6R		MTINCDVGY	27—378.4
E8L	CD8+	MSAPFDSVFY	21.6—336.8
F13L		YQNHGFVSF	6.0—406.9
H3L		FTTPLISFF	42.8—478.4
L1R		QYLLTMFF	78.3—252.8
M1R		ILAALFMYY	33.5—490.9
A29L		EVLFRLENHAETLRA	63.87—329.5
A35R		KRVIGLCIRISMVIS	61.2—412.01
A42R		LKPLIGQKFCIVYTNSL	24.83—395.86
B6R		GGVIHLSCKSGFTLT	173.03—394.33
E8L	CD4+	PSTLDYFTYLGTTINHS	37.74—412.79
F13L		FKAFNSAKNSWLNLC	13.58—184.32
H3L		YPGVMYTFTTPLISF	11.45—85.41
L1R		SLMRFKKESALATTAID	10.33—420.48
M1R		MFTAALNIQTSVNTV	15.59—412.28

Table 4. Population coverage of individual T-cell epitopes encoded in the mRNA vaccine constructs

Epitope	World	East Africa	West Africa	North Africa	South Africa	Central Africa	Southeast Asia
CD4+ A29L	63.74%	50.30%	54.75%	59.37%	7.65%	47.53%	47.99%
CD4+ A35R	66.41%	57.36%	56.40%	60.49%	7.65%	52.75%	50.93%
CD4+ A42R	62.96%	31.28%	46.50%	53.28%	7.65%	38.22%	40.23%
CD4+ B6R	60.37%	53.35%	48.59%	51.52%	32.10%	46.19%	42.57%
CD4+ E8L	66.73%	43.60%	49.05%	53.33%	1.79%	34.42%	46.96%
CD4+ F13L	70.55%	53.08%	57.74%	60.85%	7.65%	49.06%	48.55%
CD4+ H3L	72.95%	59.93%	59.33%	61.95%	7.65%	54.20%	51.48%
CD4+ L1R	66.73%	43.60%	49.05%	53.33%	1.79%	34.42%	46.96%
CD4+ M1R	70.55%	53.08%	57.74%	60.85%	7.65%	49.06%	48.55%
CD4+ set in mBThPox	***81.81%***	***68.30%***	***65.23%***	***75.06%***	***32.10%***	***62.71%***	***56.98%***
CD8+ A29L	29.38%	41.21%	59.50%	41.33%	31.93%	42.87%	21.03%
CD8+ A35R	18.52%	18.92%	31.44%	18.28%	19.24%	22.19%	6.90%
CD8+ A42R	11.72%	12.32%	11.30%	6.42%	6.09%	8.36%	17.35%
CD8+ B6R	42.23%	33.06%	48.97%	33.93%	39.75%	33.14%	52.67%
CD8+ E8L	37.74%	35.28%	45.32%	32.68%	34.99%	37.00%	21.76%
CD8+ F13L	32.60%	23.10%	47.63%	35.34%	24.35%	30.06%	35.55%
CD8+ H3L	32.88%	42.67%	50.89%	35.57%	32.99%	37.61%	30.33%
CD8+ L1R	26.18%	17.08%	31.79%	26.56%	25.59%	19.95%	40.17%
CD8+ M1R	43.99%	26.95%	40.41%	29.53%	35.32%	33.61%	41.44%
CD8+ set in mTcPox	***77.67%***	***68.9%***	***82.72%***	***72.70%***	***76.02%***	***67.23%***	***85.69%***

The T-cell epitopes encoded by the couplet mRNA constructs can potentially dock within the peptide-binding groove of HLA

The epitopes encoded in the mRNA construct were docked to the PDB structures of their weakest (highest IC_{50} value) HLA allele binders. This step was conducted to support the binding data obtained from T-cell epitope prediction tools employed in this research. As depicted in Figures 1 and 2, each candidate epitope docks within the peptide-binding groove of the HLA I and HLA II molecules, respectively.

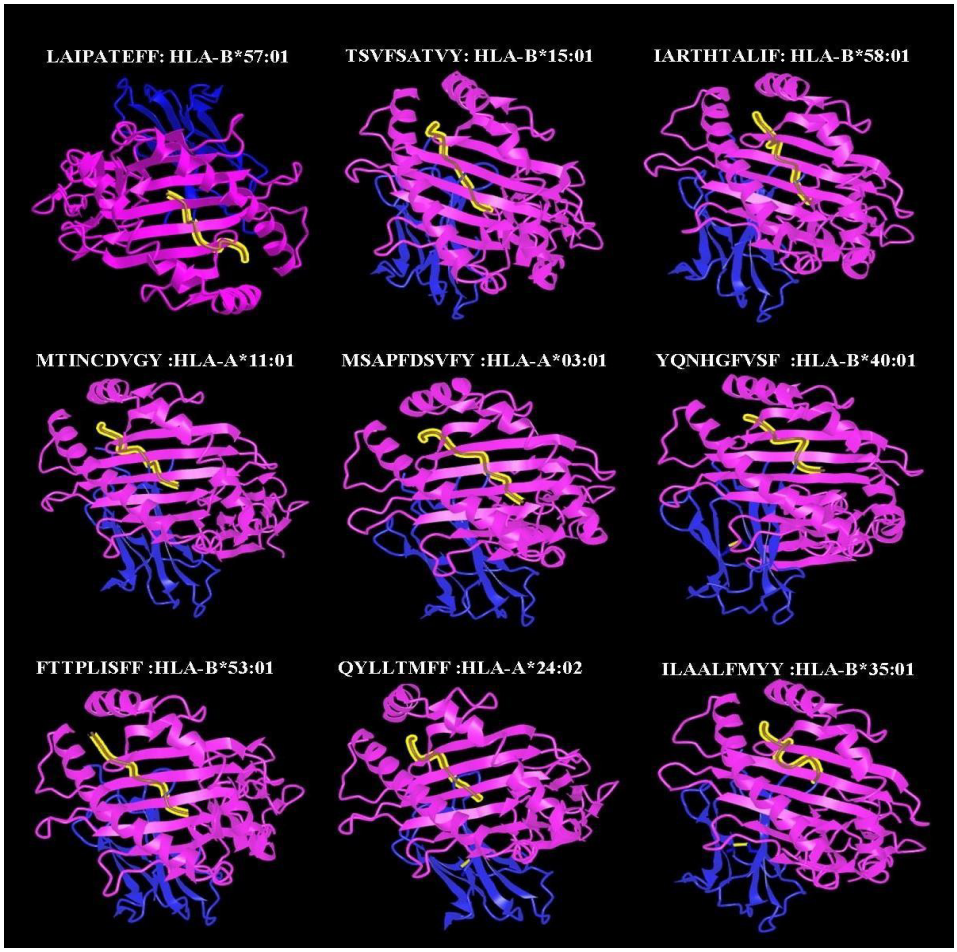

Figure 1. The structure models of CD8+ epitopes docked with the predicted HLA I allele binders. The HLA chains are depicted in blue and magenta while the epitopes docked within the peptide-binding groove are depicted in yellow.

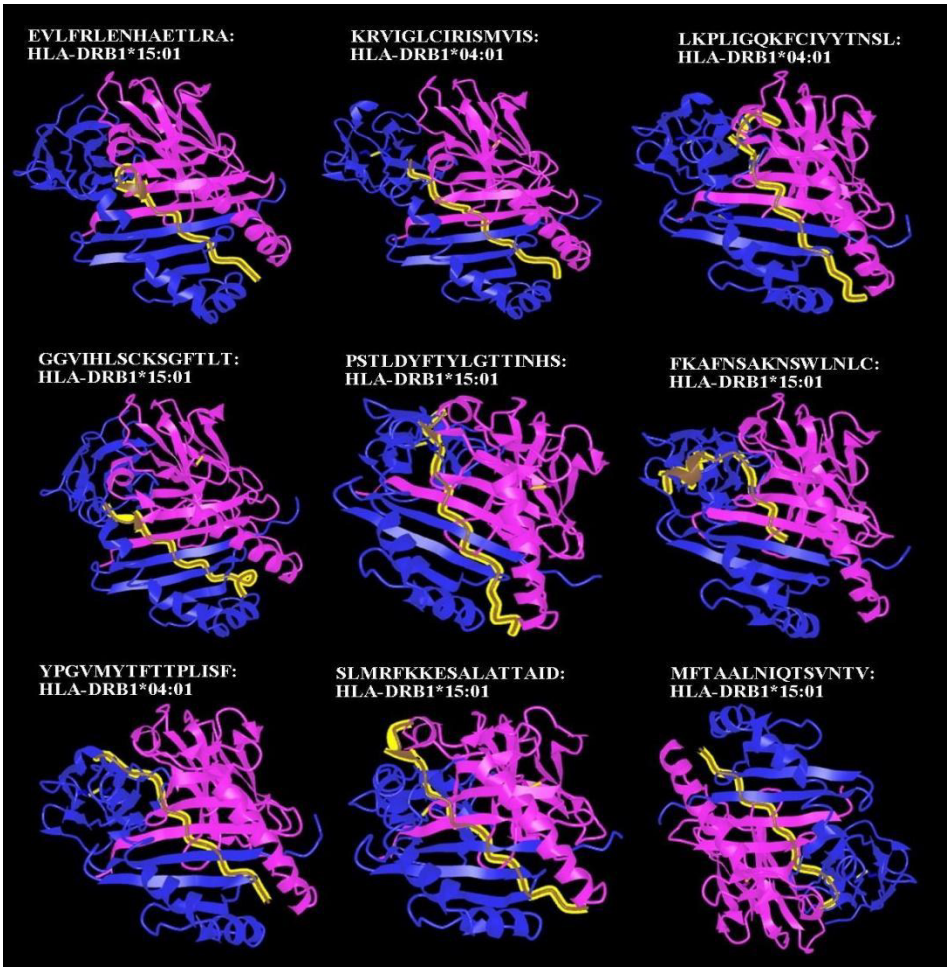

Figure 2. The structure models of CD4+ epitopes docked with the predicted HLA II allele binders. The HLA chains are depicted in blue and magenta while the epitopes docked within the peptide-binding groove are depicted in yellow.

The estimated accuracy (EA) of the initial PDB structures were tabulated in Table 5. For each docked complex, generated PDB structures having an EA of < 1.0 were further refined, while those with accuracy of 1.0 were directly utilized. The percentage of Rama favored residues for the refined structures (RR) were higher than the initial (unrefined) PDB structures (RI), supporting the necessity and the efficacy of refinement steps conducted in this study for structures with EA of < 1.0. The dissociation constant (K_D) and the Gibbs free energy of complex formation (ΔG_{bind}) at 37 ^{0}C, are also indicated in Table 5.

Table 5. The summary of modeling accuracy and binding properties of epitope-HLA structure complexes

Epitope	Weakest HLA binder	IC_{50}	PDB ID	EA	RI	RR	ΔG_{Bind}	K_D
LAIPATEFF	B*57:01	139.6	6BXQ	1	NA	NA	-8.8	6.70E-07
TSVFSATVY	B*15:01	155.6	8ELH	1	NA	NA	-12.5	1.50E-09
IARTHTALIF	B*58:01	175.1	5VWH	1	NA	NA	-10	8.50E-08
MTINCDVGY	A*11:01	378.4	7M8T	1	NA	NA	-9.6	1.60E-07
MSAPFDSVFY	A*03:01	336.8	7L1B	1	NA	NA	-11.4	8.70E-09
YQNHGFVSF	B*40:01	406.9	6IEX	0.981	98.1	98.1	-9.7	1.40E-07
FTTPLISFF	B*53:01	478.4	7R7V	1	NA	NA	-11.2	1.30E-08
QYLLTMFF	A*24:02	252.8	6XQA	0.978	98.7	98.7	-10.3	5.60E-08
ILAALFMYY	B*35:01	490.9	4LNR	1	NA	NA	-11.5	7.30E-09
EVLFRLENHAETLRA	DRB1*15:01	329.5	IBX2	0.846	97.4	99.2	-12.1	3.00E-09
KRVIGLCIRISMVIS	DRB1*04:01	412.01	5NI9	0.903	98.4	99	-11.8	4.50E-09
LKPLIGQKFCIVYTNSL	DRB1*04:01	395.86	5NI9	0.883	98.4	98.7	-13.3	4.10E-10
GGVIHLSCKSGFTLT	DRB1*15:01	394.33	IBX2	0.887	98.9	99.4	-12.4	1.90E-09
PSTLDYFTYLGTTINHS	DRB1*15:01	412.79	IBX2	0.944	98.2	98.4	-13.4	3.70E-10
FKAFNSAKNSWLNLC	DRB1*15:01	184.32	IBX2	0.888	98.4	98.4	-11.2	1.20E-08
YPGVMYTFTTPLISF	DRB1*04:01	85.41	5NI9	0.954	97.6	99	-10.7	3.00E-08
SLMRFKKESALATTAID	DRB1*15:01	420.48	IBX2	0.85	98.7	98.7	-12.1	3.10E-09
MFTAALNIQTSVNTV	DRB1*15:01	412.28	IBX2	0.848	97.9	98.4	-12.6	1.30E-09

***Footnote**: EA is the estimated accuracy. RI (8th column) is the percentage of Rama favored residues in the initial structure and RR (9th column) is the percentage of Rama favored residues in the initial structure. IC_{50}, K_D, and ΔG_{bind}, are expressed in nM, M, and kcal/mol, respectively.*

The couplet mRNA constructs contain adjoined elements and epitopes directed to endogenous and exogenous pathways

Nine selected candidate CD8+ T-cell epitopes were arranged in order to maximize the cleavage scores of epitopes. Sequence of the protein product of mTcPox contains 82 residues (MTINCDVGYFTTPLISFFMSAPFDSVFYIAR THTALIFQYLLTMFFTSVFSATVYILAALFMYYLAIPATEFFYQNHGFVSF). It has a molecular weight of 9496.09 Da, pI of 5.20, aliphatic index of 89.27, and grand average of hydropathicity (GRAVY) index of 0.940. Its extinction coefficient (M^{-1} cm^{-1}) in water at 280 nm is 10430 assuming all pairs of Cys residues form

cystines, and 10430 assuming all Cys residues are reduced. Its estimated half-life is 30 hours in mammalian reticulocytes, in vitro. The instability index is computed to be 38.3 which classified the protein as stable. The cleavage scores of adjoined cytotoxic T-cell epitopes are shown in Table 6.

Table 6. The immunoproteosome cleavage scores of adjoined CD8+ epitopes in the mTcPox construct

Adjacent CD8+ T-cell epitopes	Immunoproteosome score
MTINCDVGY—FTTPLISFF	0.5310
FTTPLISFF—MSAPFDSVFY	0.5199
MSAPFDSVFY—IARTHTALIF	0.5557
IARTHTALIF—QYLLTMFF	0.6519
QYLLTMFF—TSVFSATVY	0.8407
TSVFSATVY—ILAALFMYY	0.5557
ILAALFMYY—LAIPATEFF	0.6021
LAIPATEFF—YQNHGFVSF	0.4258

The protein product of mBThPox construct contains 257 residues and was designed to express the human renin signal sequence. Figure 3 shows the sequence of the product of the construct. The amino acid residues highlighted in yellow, gray, blue, green, and orange, are the human renin signal sequence, the series of adjoined CD4+ T-cell epitopes, the B-cell peptide (P1) spanning residues 146-178 of A35R, the B-cell peptide (P2) spanning 115th to 143rd residue of A35R, and the B-cell peptide (P3) covering residues 23-45 of the B6R, respectively. Letters in lower case represent the linkers used in concatenating the three B-cell peptides.

Figure 3. Sequence of the protein product of mBThPox construct.

The predicted signal cleavage site for SecSPI is between positions 23 and 24, with the probability of 0.943327 and likelihood of 0.9988. This cleavage site is located exactly between the last residue of the human renin signal sequence and the first residue of the first CD4+ epitope included in the construct (PSTLDYFTYLGTTINHS). The likelihood that it is not GPI-anchored is 0.995. The next crucial step is to determine whether the designed CD4+ epitopes can be recognized and cleaved by known epitope-generating proteases (cathepsins D, L, and G) of the exogenous pathway. The candidate helper T-cell epitopes were arranged to maximize cathepsin D, L and G cleavage scores of C-terminus residue of each epitope (Table 7).

Table 7. The cathepsin cleavage scores of adjoined CD4+ T-cell epitopes in mBThPox construct

Adjoined CD4+ epitopes	Cleavage scores	Cathepsin
PSTLDYFTYLGTTINHS/GGVIHLSCKSGFTLT	0.212	G
GGVIHLSCKSGFTLT/KRVIGLCIRISMVIS	0.706	L
KRVIGLCIRISMVIS/YPGVMYTFTTPLISF	0.616	L
YPGVMYTFTTPLISF/MFTAALNIQTSVNTV	0.892	D
	0.873	G
MFTAALNIQTSVNTV/SLMRFKKESALATTAID	0.377	G
SLMRFKKESALATTAID/LKPLIGQKFCIVYTNSL	0.723	L
LKPLIGQKFCIVYTNSL/EVLFRLENHAETLRA	0.581	D
EVLFRLENHAETLRA/FKAFNSAKNSWLNLC	0.616	D
FKAFNSAKNSWLNLC/kkDYVEDTWGSDGNPITKTTS DYQDSDVSQEVRKY (KK linker and P1)	0.621	L

The protein structure model of its product was generated and utilized to assess the accessibility of adjoined B-cell epitopes in the mBThPox construct. The three peptide sequences (P1, P2, and P3) cover all 18 candidate B-cell epitopes identified in this study. Two peptides from A35R and 1 peptide from

B6R sequence were arranged and linked using KK and AAY linkers to maximize the accessibility of B-cell epitopes in the structure. The Ramachandran plot analysis of the model structure generated in this study, indicates that the percentage of residues in the highly preferred conformation increased from 93.1% to 94.7%, after structural refinement. Moreover, the clash score of the model structure was reduced from 17.0 to 12.2. The overall quality (ERRAT score) of the refined structure is 88.4298.

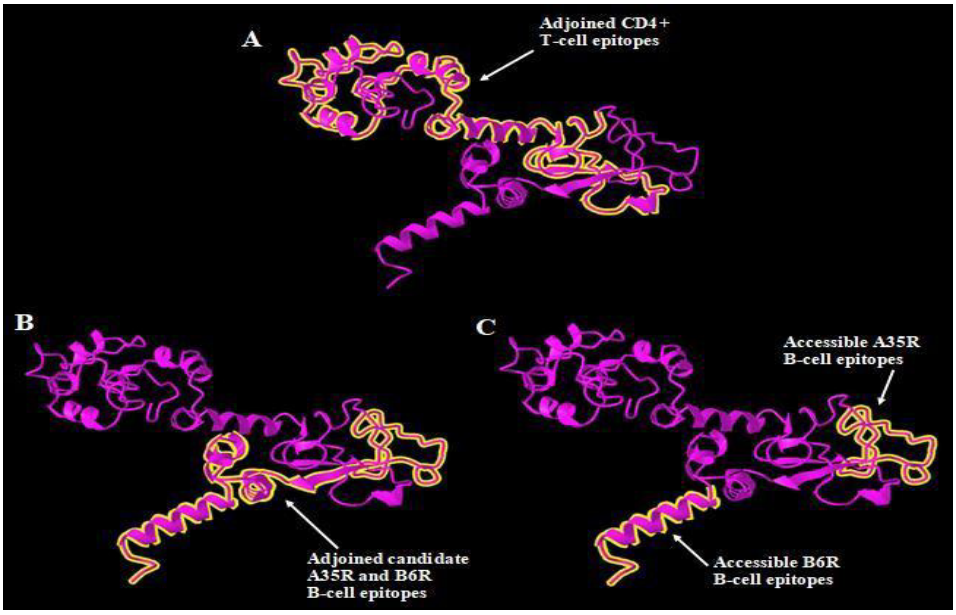

Figure 4. Structure model generated for the protein product of mBThPox construct. Topographical positions of adjoined CD4+ T-cell epitopes (A), adjoined candidate B-cell epitopes (B), and accessible A35R and B6R B-cell epitopes (C) in the model structure are highlighted in yellow.

Structural B-cell epitope analysis in Ellipro predicted the following accessible positions in the generated protein model: 162-198 and 23-257 as linear B-cell epitopes while residues 162-197, 218-225, and 237-257 as structural B-cell epitopes. Out of 18 candidate B-cell epitopes mapped in the study, 8 candidate B-cell epitopes (Table 8) were predicted to be accessible in the protein structure of the vaccine, all of which are accessible both as linear and structural B-cell epitopes. Five and three B-cell epitopes are from A35R and B6R Mpox EEV proteins, respectively. Figure 4 depicts the positions of epitopes in the model

structure generated for the protein product of mBThPox. Moreover, results from the secondary structure analysis imply that the product is made up primarily of random coils (46.69%), and the series of adjoined candidate B-cell epitopes (167 to 257) is located in regions rich in random coils and extended strands.

Table 8. Accessible candidate B-cell epitopes encoded in mBThPox construct

Antigen	Accessible sequences in the model structure	Position in the construct	Accessible candidate B-cell epitopes
A35R	DYVEDTWGSDGNPITKT TSDYQDSDVSQEVRK	162-198	TKTTSDYQDSDVSQEV ITKTTSDYQDSDV TWGSDGNPITKTTSDYQDSDVSQEV EDTWGSDGNPITKTTSDYQDSDVS EDTWGSDGNPITKTTS
B6R	TMNNAKLTSTETSFND KQKVT	237-257	AKLTSTETSFNDKQKV KLTSTETSFNDKQKVT LTSTETSFNDK

Evaluation of the physicochemical properties of the product of mBThPox showed that the protein has a pI of 8.80, molecular weight of 28795.96 Da and aliphatic index of 78.95. Its grand average of hydropathicity (GRAVY) score (-0.140) indicates that the product has more tendency to interact in a hydrophilic environment. The extinction coefficients (M^{-1} cm^{-1}) measured in water at 280 nm are 49765, assuming all pairs of Cys residues form cystines; and 49390, assuming all Cys residues are reduced. Its estimated half-life in mammalian reticulocytes in vitro is 30 hours. The instability index of the product is 31.96, which classified the protein as stable.

The optimized sequences of Mpox couplet mRNA vaccine

The optimized mRNA sequences of mTcPox (A) and mBThPox (B) constructs are shown in Figure 5. The RNA sequence of mTcPox and mBThPox, has a GC content of 57.83% with CAI of 0.99 and a GC content of 61.76% with CAI of 1.0 in humans, respectively. The estimated minimum free energy change of RNA folding for mTcPox and mBThPox at 37 ^{0}C, are -90.10 kcal/mol and -292.90 kcal/mol, respectively.

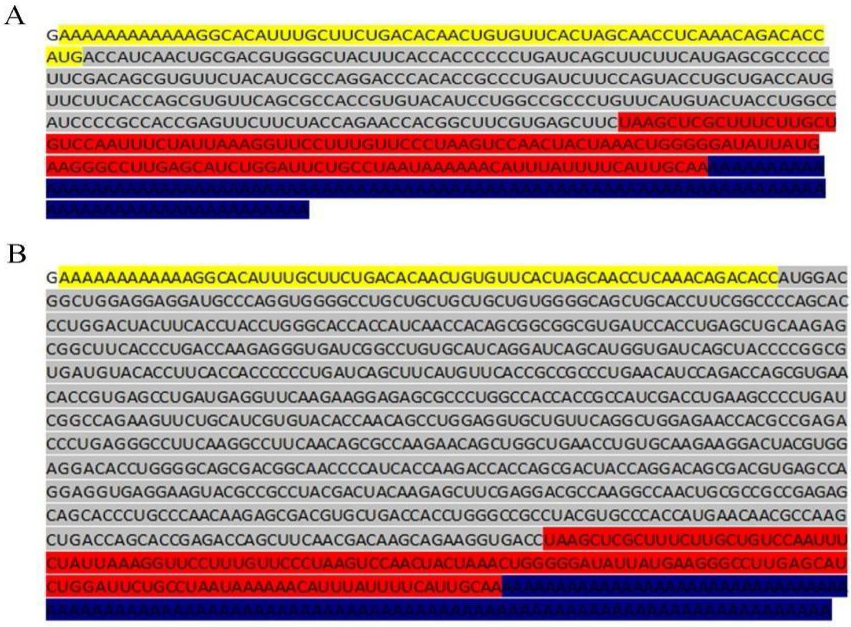

Figure 5. mRNA sequences of the Mpox couplet vaccine. The RNA sequence of mTcPox (A) contains 549 nt while mBThPox (B) has 1074 nt. Both sequences begin with the conventional 5' cap (m7GpppN1m). The 5' UTR sequence of *Homo sapiens* beta-globin which includes the 12 A nucleotides and the Kozak consensus sequence (GGC), is highlighted in yellow. Adjacent to it is the open reading frame (highlighted in gray), followed by the stop codon in the 3' UTR beta-globin sequence (highlighted in red), and a 100-nucleotide poly (A) tail in blue.

Discussion

The declaration of Mpox as a Public Health Emergency of International Concern highlights the urgent need for prevention. Current vaccines use vaccinia, a virus similar to smallpox. JYNNEOS, a third-generation, non-replicating vaccine, shows 85.9% efficacy (95% CL, 73.8–92.4) with fewer adverse reactions (Dalton *et al.,* 2023). ACAM2000, a second-generation vaccine, is replication-competent and linked to more severe side effects. About 95% of recipients develop neutralizing antibodies post-vaccination. LC16, another third-generation vaccine, uses a live attenuated Lister strain; its efficacy is still under study (Wahid *et al*., 2025). Given the limited protection and adverse reactions, Mpox-specific vaccine development is urgently needed.

mRNA vaccine technology offers key advantages over conventional formulations. Notably, mRNA vaccines are safer as they lack live virus and are easily eliminated by the body. They also allow faster development and manufacturing (Koppu *et al*., 2022). This study aimed to design a couplet mRNA vaccine against Mpox disease via immunoinformatics for a streamlined, cost-effective approach. The vaccine includes epitopes that can be potentially recognized by B and T lymphocytes, enabling targeted immune responses. Epitope-based vaccines offer specificity and potency while minimizing biohazard risks (Hajissa *et al*., 2019). Epitope processing varies by type: cytotoxic T-cell epitopes follow the endogenous pathway and are presented via MHC I, while helper T-cell epitopes use the exogenous pathway and are presented by antigen-presenting cells through MHC II. B-cell epitopes bind to B-cell receptors (BCRs), are processed exogenously, and presented to T-cell receptors (TCRs) to activate naive B cells (Blum *et al.,* 2013). The couplet mRNA vaccine includes two constructs: mTcPox (CD8+ T-cell epitopes via endogenous pathway) and mBThPox (B-cell and CD4+ T-cell epitopes via exogenous pathway). This design enhances epitope presentation and immune response. Targeting nine virulent Mpox antigens (A29L, A35R, A42R, B6R, E8L, F13L, H3L, L1R, and M1R) supports a multi-targeted, cost-effective vaccine strategy.

All candidate epitopes obtained in this study possess Shannon variability scores ≤ 0.1, implying high conservancy of the identified epitopes. Its application was validated by utilizing > 500 sequences per Mpox antigen of the same length. These numbers are higher than the required minimum number of sequences (100) to meet the assumption in indicating conservancy using the Shannon variability index (Garcia-Boronat *et al*., 2008). Results from conservancy analysis showed that the full-length sequence of Mpox A42R is highly conserved, while all the other antigens contain at least 1 variable amino acid. F13L has the highest number of variable residues (6) among the Mpox antigens investigated in this study. Nevertheless, these results imply that the sequences of the 9 Mpox antigens are conserved, as there are only few residues with Shannon variability scores > 0.1. Using the highly conserved sequences for epitope mapping is a pivotal step to avoid epitope immune evasion. The highly conserved cytotoxic and helper T-cell epitopes possess acceptable to high binding affinity, as indicated by IC_{50} values ranging from 499.9 to 2.9 nM. Epitopes with IC_{50} < 50 nM and < 500 nM are classified to have high affinity and intermediate binding, respectively (Wu *et al*., 2019).

The ability to induce immunogenicity is an essential property for epitopes included in any vaccine formulation. In this study, the potentially immunogenic cytotoxic T-cell epitopes were identified through the combination of immunogenicity scores generated from 5 experimentally validated CD8+ T-cell epitopes. This

step was conducted due to the current lack of consensus immunogenicity threshold that can be used in immunogenicity tools to distinguish immunogenic from non-immunogenic cytotoxic T-cell epitopes. This strategy may reduce bias by relying on the combination of immunogenicity scores generated from multiple experimentally validated epitopes using multiple state-of-the-art immunogenicity tools, rather than just utilizing a single immunogenicity tool.

Interferon-gamma (IFN-γ) is a key cytokine in promoting the differentiation and function of naive helper T cells (Th0) to Th1 cells, essential for fighting intracellular pathogens, such as Mpox viruses. Interleukin-4 (IL4) is another type of cytokine that induces the activation and differentiation of Th0 to Th2 cells which is crucial in promoting the activation and function of B cells (Aguiar *et al.,* 2024). The candidate CD4+ epitopes generated by this study are classified as IFN-γ and IL4 inducers, implying that the epitopes can potentially induce activation of both Th1 and Th2 cells to fight Mpox-infected cells and activate B cells for antibody production against extracellular Mpox viruses. Overall, 559 candidate CD4+ and 104 candidate CD8+ T-cell epitopes from the nine virulent Mpox antigens were obtained by this study through immunoinformatics approach.

Global concern over Mpox began with its high burden in Africa, marked by rising cases, fatalities, and international spread (Ndembi *et al*., 2025). Although Southeast Asia (SEA) currently has lower prevalence, the emergence of clade Ib poses risks to regions affected by clade IIb (A *et al*., 2025). Strategic development of immunotherapeutics is essential. The WHO recommends 80% population coverage for orthopoxvirus eradication via vaccination (Taube *et al*., 2023). This study estimates that selected CD8+ and CD4+ T-cell epitopes cover 77.67% and 81.81% globally, 92.77% and 75.06% in Africa, and 90.87% and 56.98% in SEA. South Africa shows the lowest CD4+ coverage (32.1%), but CD8+ epitopes compensate with 88.79%. To optimize mRNA vaccine coverage, epitopes with highest global reach were selected: mTcPox covers 81.81%, meeting WHO's target, while mBThPox covers 77.67%, falling short by under 3%. However, this doesn't imply ineffectiveness, as Mpox is less fatal than smallpox and may require lower coverage. The selected epitopes are promiscuous, enabling broader population reach. Actual coverage may exceed estimates, as some HLA alleles were excluded from IEDB Population Coverage tool calculations.

T-cell epitopes encoded in the couplet mRNA constructs were docked to their weakest HLA allele binder. Analysis of the quality of PDB structure models generated for the docked complex showed a high percentage of Rama favored residues and high accuracy. These results supported the use of generated model structures in subsequent evaluation steps. Molecular docking analysis revealed that the selected candidate epitopes bind exactly to the peptide binding groove of the HLA molecule. The favorability of complex formation can be measured

using the equilibrium K_D, wherein smaller K_D indicates favorable binding. In biochemical systems, a complex with K_D value < 1.0e-07 M, is considered to have a high binding affinity (Yewdell, 2022). Docking analysis revealed that the K_D values of complexes formed are all lower than 1.0e-07 M, despite docking with its weakest HLA binder. Moreover, ΔG_{bind} values of the docked complexes range from -8.8 to -13.4 kcal/mol. This is lower than the most commonly used ΔG_{bind} value (-6.0 kcal/mol) for the selection of potential candidates in drug design (Ivanova *et al*., 2022). These results further support the potential immunogenicity of candidate T-cell epitopes mapped in this study.

The Mpox virus has two infectious forms: extracellular enveloped virion (EEV) and intracellular mature virion (IMV). EEV drives transmission and has three surface proteins: A35R (type II membrane protein), B6R (glycoprotein regulating the complement system), and F13L/CL19 (inner surface protein) (Sagdat *et al*., 2024). F13L was excluded from B-cell epitope mapping due to its buried location. A35R and B6R are neutralizing and ideal vaccine targets (Yang *et al.,* 2025). Epitope mapping considered flexibility, accessibility, hydrophilicity, secondary structure, and antigenicity. All candidate epitopes are in conserved, external regions of A35R and B6R, allowing BCR binding. Predicted epitopes with post-translational modifications (PTMs) were excluded, as unmodified vaccine residues may hinder recognition. None of the 18 candidate epitopes contain PTM residues.

Arrangement of nine candidate CD8+ T-cell epitopes in mTcPox construct showed, that each cytotoxic epitope can be cleaved and generated with high probability, as indicated by immunoproteosome cleavage scores > 0.5000, except for the last epitope (YQNHGFVSF) which has an immunoproteosome score of 0.4258. Investigation of its physicochemical properties in silico, suggest that the product is stable in vitro, with relatively longer half-life in mammalian cells, and a preference for interactions with hydrophobic systems.

Results from the *in silico* analysis suggest the mBThPox protein is secreted via the Sec translocon and cleaved by Signal Peptidase I (SecSPI), without membrane anchoring. Its CD4+ epitopes are predicted to be processed by cathepsins D, L, and G in the exogenous pathway. KK and AAY linkers were found to enhance B-cell epitope accessibility and were used to join three peptides covering 18 candidate epitopes. The modeled protein structure is high quality, with >90% residues in favored conformations and an ERRAT score >50% (Gupta *et al*., 2013; Lombard *et al*., 2024). Eight B-cell epitopes (5 from A35R, 3 from B6R) are accessible as linear and structural epitopes. However, detection may be limited by the PDB model, Ellipro tool, and study thresholds. The remaining nine epitopes might be identified using alternative prediction tools with relaxed criteria. Physicochemical analysis indicates the protein is stable with a half-life >24 hours in human reticulocytes.

This study recommends using a conventional 5' cap (m7GpppN1m) with a 7-methylguanosine moiety to protect mRNA from exonuclease degradation and enhance splicing, nuclear export, and translation (Gote *et al*., 2023). The 5' UTR of human beta-globin improves translational efficiency in mRNA vaccines (Ma *et al*., 2024). Incorporating a Kozak sequence and 12 adenosines (polyA) into the leader sequence boosts translation and prevents secondary structure formation at the 5' end, as shown in poxvirus mRNA (Dhungel *et al*., 2017). The 3' UTR of human beta-globin increases protein yield and mRNA stability (Adibzadeh *et al*., 2019), while a 100-nucleotide poly(A) tail further enhances stability (Vélez *et al*., 2025). The couplet mRNA vaccines (mTcPox and mBThPox) show high potential for human expression, with CAI values of 0.99 and 1.00, respectively. Optimal GC content may protect against endoribonuclease degradation and prolong mRNA lifespan (Leong *et al*., 2025). Structural analysis reveals that neither mRNA begins with a hairpin loop, facilitating efficient ribosome binding. Their minimum free energy (MFE) values support stable folding and accessibility for translation.

More than its sophisticated design and promising efficacy, the B-cell and T-cell epitopes that can be expressed and generated from the Mpox couplet mRNA vaccine, exhibited very low probability of causing adverse reactions due to cross-reactivity with human proteomes, allergic reactions, and toxicity. Results from in silico safety profile evaluation suggest its safety for future Mpox vaccine clinical applications.

Conclusions

This study offers a novel and specific couplet mRNA vaccine design for future research and vaccine development against the PHEIC disease-causing Mpox virus. Leveraging computational immunology enables efficient, cost-effective discovery of immunotherapeutics for infectious diseases like Mpox. However, its application demands caution due to some inherent assumptions and restrictions. A limited set of validated cytotoxic epitopes was used to establish thresholds for excluding non-immunogenic candidates, highlighting the need to refine consensus immunogenicity values across tools. Overall, this is the first strategic design of a couplet mRNA vaccine containing potentially immunogenic B-cell and T-cell epitopes against multiple Mpox antigens. Safety assessments *in silico* suggest that it can be administered in humans with very minimal adverse reactions. Further *in vitro*, animal, and clinical studies are anticipated.

Ethical Approval
This study did not conduct procedures involving human participants, samples and data; thus, ethics approval was not deemed necessary.

Declaration of Conflict of Interest
The author declares no conflict of interest.

References

A, J., Gan, G., Endo, A., Jin Tan, R. K., Prem, K., & Dickens, B. L. (2025). Is Southeast Asia and the Western Pacific ready for potential monkeypox virus outbreaks?. *The Lancet regional health. Western Pacific,* 57, 101526. https://doi.org/10.1016/j.lanwpc.2025.101526

Adibzadeh, S., Fardaei, M., Takhshid, M. A., Miri, M. R., Rafiei Dehbidi, G., Farhadi, A., Ranjbaran, R., Alavi, P., Nikouyan, N., Seyyedi, N., Naderi, S., Eskandari, A., & Behzad-Behbahani, A. (2019). Enhancing Stability of Destabilized Green Fluorescent Protein Using Chimeric mRNA Containing Human Beta-Globin 5' and 3' Untranslated Regions. *Avicenna J Med Biotechnol,* 11(1), 112–117. https://pmc.ncbi.nlm.nih.gov/articles/PMC6359690/

Aguiar MPd & Vieira JH. (2024). Entrance to the multifaceted world of CD4+ T cell subsets. *Explor Immunol,* 4, 152–68. https://doi.org/10.37349/ei.2024.00134

Beeson, A., Styczynski, A., Hutson, C. L., Whitehill, F., Angelo, K. M., Minhaj, F. S., Morgan, C., Ciampaglio, K., Reynolds, M. G., McCollum, A. M., & Guagliardo, S. A. J. (2023). Mpox respiratory transmission: the state of the evidence. *Lancet Microbe*, 4(4), e277–e283. https://doi.org/10.1016/S2666-5247(23)00034-4

Blum, J. S., Wearsch, P. A., & Cresswell, P. (2013). Pathways of antigen processing. *Annu Rev Immunol*, 31, 443–473. https://doi.org/10.1146/annurev-immunol-032712-095910

Bogacka, A., Wroczynska, A., Rymer, W., Grzesiowski, P., Kant, R., Grzybek, M., & Parczewski, M. (2025). Mpox unveiled: Global epidemiology, treatment advances, and prevention strategies. *One Health*, 20, 101030. https://doi.org/10.1016/j.onehlt.2025.101030

Callaby, H., Belfield, A., Otter, A. D., Atkinson, B., Reynolds, M., Roberts, H., & Gordon, N. C. (2025). Mpox: current knowledge and understanding-a scoping review. *FEMS Microbiol Rev*, 49, fuaf025. https://doi.org/10.1093/femsre/fuaf025

Dalton, A. F., Diallo, A. O., Chard, A. N., Moulia, D. L., Deputy, N. P., Fothergill, A., Kracalik, I., Wegner, C. W., Markus, T. M., Pathela, P., Still, W. L., Hawkins, S., Mangla, A. T., Ravi, N., Licherdell, E., Britton, A., Lynfield, R., Sutton, M., Hansen, A. P., Betancourt, G. S., ... CDC Multijurisdictional Mpox Case Control Study Group (2023). Estimated Effectiveness of JYNNEOS Vaccine in Preventing Mpox: A Multijurisdictional Case-Control Study - United States, August 19, 2022-March 31, 2023. *MMWR Morb Mortal Wkly Rep*, 72(20), 553–558. https://doi.org/10.15585/mmwr.mm7220a3

Dhanda, S. K., Vir, P., & Raghava, G. P. (2013). Designing of interferon-gamma inducing MHC class-II binders. *Biol Direct*, 8, 30. https://doi.org/10.1186/1745-6150-8-30

Dhungel, P., Cao, S., & Yang, Z. (2017). The 5'-poly(A) leader of poxvirus mRNA confers a translational advantage that can be achieved in cells with impaired cap-dependent translation. *PLoS Pathog*, 13(8), e1006602. https://doi.org/10.1371/journal.ppat.1006602

Du, Z., Xu, Y., Liu, C., & Li, Y. (2024). pLM4Alg: Protein Language Model-Based Predictors for Allergenic Proteins and Peptides. *J. Agric. Food Chem.*, 72(1), 752–760. https://doi.org/10.1021/acs.jafc.3c07143

Garcia-Boronat, M., Diez-Rivero, C. M., Reinherz, E. L., & Reche, P. A. (2008). PVS: a web server for protein sequence variability analysis tuned to facilitate conserved epitope discovery. *Nucleic Acids Res.*, 36(Web Server issue), W35–W41. https://doi.org/10.1093/nar/gkn211

Gfeller, D., Schmidt, J., Croce, G., Guillaume, P., Bobisse, S., Genolet, R., Queiroz, L., Cesbron, J., Racle, J., & Harari, A. (2023). Improved predictions of antigen presentation and TCR recognition with MixMHCpred2.2 and PRIME2.0 reveal potent SARS-CoV-2 CD8+ T-cell epitopes. *Cell Syst.*, 14(1), 72–83.e5. https://doi.org/10.1016/j.cels.2022.12.002

Gote, V., Bolla, P. K., Kommineni, N., Butreddy, A., Nukala, P. K., Palakurthi, S. S., & Khan, W. (2023). A Comprehensive Review of mRNA Vaccines. *Int. J. Mol. Sci.*, 24(3), 2700. https://doi.org/10.3390/ijms24032700

Gupta, C. L., Akhtar, S., Bajpaib, P., Kandpal, K. N., Desai, G. S., & Tiwari, A. K. (2013). Computational modeling and validation studies of 3-D structure of neuraminidase protein of H1N1 influenza A virus and subsequent in silico elucidation of piceid analogues as its potent inhibitors. *EXCLI J.*, 12, 215–225

Hajissa, K., Zakaria, R., Suppian, R., & Mohamed, Z. (2019). Epitope-based vaccine as a universal vaccination strategy against Toxoplasma gondii infection: A mini-review. *J. Adv. Vet. Anim. Res.*, 6(2), 174–182. https://doi.org/10.5455/javar.2019.f329

Ho, L. L. Y., Schiess, G. H. A., Miranda, P., Weber, G., & Astakhova, K. (2024). Pseudouridine and N1-methylpseudouridine as potent nucleotide analogues for RNA therapy and vaccine development. *RSC Chem. Biol.*, 5(5), 418–425. https://doi.org/10.1039/d4cb00022f

Ivanova, L., & Karelson, M. (2022). The Impact of Software Used and the Type of Target Protein on Molecular Docking Accuracy. *Molecules*, 27(24), 9041. https://doi.org/10.3390/molecules27249041

Koppu, V., Poloju, D., Puvvala, B., Madineni, K., Balaji, S., Sheela, C. M. P., Manchikanti, S. S. C., & Moon, S. M. (2022). Current Perspectives and Future Prospects of mRNA Vaccines against Viral Diseases: A Brief Review. *Int J Mol Cell Med*, 11(3), 260–272. https://doi.org/10.22088/IJMCM.BUMS.11.3.260

Leong, K. Y., Tham, S. K., & Poh, C. L. (2025). Revolutionizing immunization: a comprehensive review of mRNA vaccine technology and applications. *Virol J*, 22(1), 71. https://doi.org/10.1186/s12985-025-02645-6

Li, G., Iyer, B., Prasath, V. B. S., Ni, Y., & Salomonis, N. (2021). DeepImmuno: deep learning-empowered prediction and generation of immunogenic peptides for T-cell immunity. *Brief Bioinform*, 22(6), bbab160. https://doi.org/10.1093/bib/bbab160

Lombard, V., Grudinin, S., & Laine, E. (2024). Explaining Conformational Diversity in Protein Families through Molecular Motions. *Sci Data*, 11(1), 752. https://doi.org/10.1038/s41597-024-03524-5

Lu, J., Xing, H., Wang, C., Tang, M., Wu, C., Ye, F., Yin, L., Yang, Y., Tan, W., & Shen, L. (2023). Mpox (formerly monkeypox): pathogenesis, prevention, and treatment. *Signal Transduct Target Ther*, 8(1), 458. https://doi.org/10.1038/s41392-023-01675-2

Ma, Q., Zhang, X., Yang, J., Li, H., Hao, Y., & Feng, X. (2024). Optimization of the 5' untranslated region of mRNA vaccines. *Sci Rep*, 14(1), 19845. https://doi.org/10.1038/s41598-024-70792-x

Ndembi, N., Folayan, M. O., Komakech, A., Mercy, K., Tessema, S., Mbala-Kingebeni, P., Ngandu, C., Ngongo, N., Kaseya, J., & Abdool Karim, S. S. (2025). Evolving Epidemiology of Mpox in Africa in 2024. *N Engl J Med*, 392(7), 666–676. https://doi.org/10.1056/NEJMoa2411368

Nebangwa, D. N., Shey, R. A., Shadrack, D. M., Shintouo, C. M., Yaah, N. E., Yengo, B. N., Efeti, M. T., Gwei, K. Y., Fomekong, D. B. A., Nchanji, G. T., Lemoge, A. A., Ntie-Kang, F., & Ghogomu, S. M. (2024). Predictive immunoinformatics reveal promising safety and anti-onchocerciasis protective immune response profiles to vaccine candidates (Ov-RAL-2 and Ov-103) in anticipation of phase I clinical trials. *PLoS One*, 19(10), e0312315. https://doi.org/10.1371/journal.pone.0312315

Nibeyro, G., Baronetto, V., Folco, J. I., Pastore, P., Girotti, M. R., Prato, L., Morón, G., Luján, H. D., & Fernández, E. A. (2023). Unraveling tumor specific neoantigen immunogenicity prediction: a comprehensive analysis. *Front Immunol*, 14, 1094236. https://doi.org/10.3389/fimmu.2023.1094236

Olotu, F. A., & Soliman, M. E. S. (2021). Immunoinformatics prediction of potential B-cell and T-cell epitopes as effective vaccine candidates for eliciting immunogenic responses against Epstein-Barr virus. *Biomed J*, 44(3), 317–337. https://doi.org/10.1016/j.bj.2020.01.002

Rathore, A. S., Choudhury, S., Arora, A., Tijare, P., & Raghava, G. P. S. (2024). ToxinPred 3.0: An improved method for predicting the toxicity of peptides. *Comput Biol Med*, 179, 108926. https://doi.org/10.1016/j.compbiomed.2024.108926

Rawat, S. S., Keshri, A. K., Kaur, R., & Prasad, A. (2023). Immunoinformatics Approaches for Vaccine Design: A Fast and Secure Strategy for Successful Vaccine Development. *Vaccines*, 11(2), 221. https://doi.org/10.3390/vaccines11020221

Reardon, B., Koşaloğlu-Yalçın, Z., Paul, S., Peters, B., & Sette, A. (2021). Allele-Specific Thresholds of Eluted Ligands for T-Cell Epitope Prediction. *Mol Cell Proteomics*, 20, 100122. https://doi.org/10.1016/j.mcpro.2021.100122

Sagdat, K., Batyrkhan, A., & Kanayeva, D. (2024). Exploring monkeypox virus proteins and rapid detection techniques. *Front Cell Infect Microbiol*, 14, 1414224. https://doi.org/10.3389/fcimb.2024.1414224

Sharma, N., Patiyal, S., Dhall, A., Pande, A., Arora, C., & Raghava, G. P. S. (2021). AlgPred 2.0: an improved method for predicting allergenic proteins and mapping of IgE epitopes. *Brief Bioinform*, 22(4), bbaa294. https://doi.org/10.1093/bib/bbaa294

Taube, J. C., Rest, E. C., Lloyd-Smith, J. O., & Bansal, S. (2023). The global landscape of smallpox vaccination history and implications for current and future orthopoxvirus susceptibility: a modelling study. *Lancet Infect Dis*, 23(4), 454–462. https://doi.org/10.1016/S1473-3099(22)00664-8

Vélez, D. E., Torres, B. L., & Hernández, G. (2025). The Bright Future of mRNA as a Therapeutic Molecule. *Genes*, 16(4), 376. https://doi.org/10.3390/genes16040376

Wahid, M., Mandal, R. K., Sikander, M., Khan, M. R., Haque, S., Nagda, N., Ahmad, F., & Rodriguez-Morales, A. J. (2025). Safety and Efficacy of Repurposed Smallpox Vaccines Against Mpox: A Critical Review of ACAM2000, JYNNEOS, and LC16. *J Epidemiol Glob Health*, 15(1), 88. https://doi.org/10.1007/s44197-025-00432-8

Wu, T., Guan, J., Handel, A., Tscharke, D. C., Sidney, J., Sette, A., Wakim, L. M., Sng, X. Y. X., Thomas, P. G., Croft, N. P., Purcell, A. W., & La Gruta, N. L. (2019). Quantification of epitope abundance reveals the effect of direct and cross-presentation on influenza CTL responses. *Nat Commun*, 10(1), 2846. https://doi.org/10.1038/s41467-019-10661-8

Yadav, R., Chaudhary, A. A., Srivastava, U., Gupta, S., Rustagi, S., Rudayni, H. A., Kashyap, V. K., & Kumar, S. (2025). Mpox 2022 to 2025 Update: A Comprehensive Review on Its Complications, Transmission, Diagnosis, and Treatment. *Viruses*, 17(6), 753. https://doi.org/10.3390/v17060753

Yang, X., Guo, L., Duan, H., Fan, M., Xu, F., Chi, X., Pan, S., Liu, X., Zhang, X., Gao, P., Zhang, F., Wang, X., Guo, F., Ge, J., Ren, L., & Yang, W. (2025). Identification of neutralizing nanobodies protecting against poxvirus infection. *Cell Discov*, 11(1), 31. https://doi.org/10.1038/s41421-025-00771-7

Yewdell J. W. (2022). MHC Class I Immunopeptidome: Past, Present, and Future. *Mol Cell Proteomics*, 21(7), 100230. https://doi.org/10.1016/j.mcpro.2022.100230

Zahmatyar, M., Fazlollahi, A., Motamedi, A., Zolfi, M., Seyedi, F., Nejadghaderi, S. A., Sullman, M. J. M., Mohammadinasab, R., Kolahi, A. A., Arshi, S., & Safiri, S. (2023). Human monkeypox: history, presentations, transmission, epidemiology, diagnosis, treatment, and prevention. *Front Med*, 10, 1157670. https://doi.org/10.3389/fmed.2023.1157670